The Cool Interstellar Medium *

Alain Abergel (alain.abergel@ias.u-psud.fr)
IAS, Université Paris-Sud, Bât. 121, 91405 Orsay, France

Laurent Verstraete
IAS, Université Paris-Sud, Bât. 121, 91405 Orsay, France

Christine Joblin
CESR, CNRS-Université Paul Sabatier, 9 avenue du Colonel Roche, 31028 Toulouse, France

René Laureijs
Astrophysics Division, Research and Scientific Support Department of ESA, ESTEC, PO Box 299, 2200 AG Noordwijk, The Netherlands

Marc-Antoine Miville-Deschênes
CITA, 50 St-Georges street, Toronto, Ontario, M5S3H8, Canada

Abstract. Infrared spectroscopy and photometry with ISO covering most of the emission range of the interstellar medium has lead to important progress in the understanding of the physics and chemistry of the gas, the nature and evolution of the dust grains and also the coupling between the gas and the grains. We review here the ISO results on the cool and low-excitation regions of the interstellar medium, where $T_{\rm gas} \lesssim 500$ K, $n_{\rm H} \sim 100$ to 10^5 cm^{-3} and the electron density is a few 10^{-4}.

Keywords: Infrared: spectroscopy, photometry; ISM: gas, dust; ISM: PDR, cirrus, cold clouds; ISM: physical processes

JEL codes: D24, L60, 047

Revised: 8 November 2004

1. The cool interstellar medium

The interstellar medium (ISM) fills the volume of the Galaxy and its evolution is mostly driven by the stellar activity. It is composed primarily of gas and of a small amount (1% in mass) of submicronic dust grains. In spite of their low abundance, dust particles play a key role for the temperature and chemistry of the gas. Thus the evolution of the interstellar gas through its different phases (from proto-stellar cores to the diffuse medium and vice–versa) and of dust grains are closely related. Although shocks and winds play an important role in

* Based on observations with ISO, an ESA project with instruments funded by ESA Member States (especially the PI countries: France, Germany, the Netherlands and the United Kingdom) and with the participation of ISAS and NASA.

the vicinity of stars (Blommaert et al., Nisini et al., Peeters et al., this volume), the ISM is primarily heated by stellar radiation. It then cools off by continuum and line emission in the infrared (IR) and submillimetre (submm) range. Observations of the IR emission from the ISM hence provide important clues on the gas state, the nature of the dust particles, the interactions between the gas and the dust as well as the dynamical processes affecting the gas.

In the course of its lifecycle, the ISM assumes a number of phases described by the temperature $T_{\rm gas}$ and proton density $n_{\rm H}$ of the gas as well as the electron abundance $x_{\rm e}$. Most of the ISM mass resides in cool, mostly neutral phases - the *cool* or low-excitation ISM - where $T_{\rm gas} \lesssim 500$ K, $n_{\rm H} \sim 100$ to $10^5\,{\rm cm}^{-3}$ and $x_{\rm e}$ is a few 10^{-4}. The cool ISM encompasses *photon-dominated regions* or PDRs generated by the far-ultraviolet (FUV) stellar radiation field, shielded regions that are cold and molecular (the *cold clouds*), low-mass star forming clouds, the outskirts of massive star forming regions and the general ISM (the *diffuse* ISM seen in *cirrus* clouds). This medium is therefore widespread in the Galaxy (some 10% in volume), and observed to be structured on all scales (a few 0.01 to a few 10 pc, e.g., Falgarone et al. 1998, Miville-Deschênes et al. 2003). The cool ISM is the subject of this review while the more highly excited phases of the ISM, the regions around YSOs and late-type stars are discussed in this volume by Peeters et al., Nisini et al., Lorenzetti et al. and Blommaert et al., respectively.

The ISO mission (Kessler et al., 1996; Kessler et al., 2003) was particularly well suited for ISM studies because of the complementarity of its four instruments. The CAM (Cesarsky et al., 1996; Blommaert et al., 2003) and PHOT (Lemke et al., 1996; Laureijs et al., 2003 instruments provided sensitive broad-band IR images at high angular resolution (a few arcseconds for CAM to $\sim$ 1 arcminute for PHOT). The former also had a spectro-imaging facility, the CAM-CVF mode operating between 6 and 16 μm with a resolving power $R \sim 40$ while the latter was equipped with a grating spectrometer used in the PHOT-S mode (two channels: 2.5-4.9 μm and 5.8-11.6 μm with $R \sim 90$ and a 24×24 arcseconds aperture). On the other hand, the SWS (de Graauw et al., 1996; Leech et al., 2003) and LWS (Clegg et al., 1996; Gry et al., 2003) spectrometers combined relatively higher spectral resolution ($R \sim 200$ to 2000) and full spectral coverage (2.4-45.2 μm for the SWS and 43-197 μm for the LWS). The ISO instruments have detected a great wealth of gas lines and dust spectral features in emission or absorption. High spectral resolution measurements with SWS and LWS have been performed mostly towards moderately to highly excited regions (HII regions, planetary nebulae, PDRs and active galaxies) while less excited regions could only be observed by CAM and PHOT at

low spectral resolution or in broad bands. Thus ISO has provided a complete and unbiased IR spectroscopic census of interstellar matter highlighting the nature and properties of dust, the physical conditions of the gas as well as the major processes (UV stellar irradiation, shock waves) driving the evolution of these species. While the results on the H_2 and H_2O molecules (Habart et al., Cernicharo et al.) and the dust features of silicates and ices (Molster et al., Dartois et al.) are discussed in dedicated chapters of this volume, we focus here on the properties of gas and dust in the cool ISM. We also refer the reader to the recent review by van Dishoeck (2004).

2. The physics and chemistry of the gas

Combined observations of gas lines and dust emission proved to be a unique tool to constrain the physics and chemistry of the gas in the cool ISM (Section 2.1) and to quantify the importance of the interactions between gas and dust. These latter are most directly studied in low-excitation PDRs (Section 2.2) while gas dynamical processes are best traced in the less excited, diffuse medium (Section 2.3).

2.1. Probing Interstellar Chemistry with Spectroscopy of Gas-phase molecules

The wavelength range of the ISO spectrometers includes rotational and ro-vibrational transitions of many light interstellar molecules. The ISO spectroscopy data thus provided an important benchmark for models of chemistry. Furthermore, analysis of ISO spectra with models pointed at the dominant excitation processes and highlighted the structure of the regions observed.

A wealth of molecular lines has been found towards the Galactic centre. As detailed by Ceccarelli et al. (2002), the Sgr B2 region is a massive molecular cloud close to the Galactic centre containing numerous compact and ultra-compact HII regions and hot cores embedded in a relatively dense and warm envelope ($\sim 100\,\mathrm{K}$), while the entire complex is surrounded by a hot ($\geq 300\,\mathrm{K}$) envelope of diffuse gas ($n_\mathrm{H} \sim 10^3\,\mathrm{cm}^{-3}$). Sgr B2 is therefore an ideal target to detect molecular absorption. The detection of new absorption features has strongly constrained the abundances and the physical conditions (gas temperature and density) of the absorbing regions. Numerous rotational lines of hydrides (OH, CH, HF, H_2O, H_3O^+, NH_3, NH_2, NH) and hydrocarbons (C_3, C_4 or C_4H) have been detected in absorption by LWS (see Tables 4 and 5 of Goicoechea et al. 2004 for the complete list of lines and

references). Light hydrides such as OH, CH and H_2O were found at all positions, indicating the widespread presence of these species in molecular clouds. Lines of the $H_2O/OH/O^0$ and $NH_3/NH_2/NH$ sequences were found to trace the importance of photodissociation processes and shock respectively (Goicoechea et al. 2004). The HD molecule has been detected by the LWS (Wright et al. 1999, Caux et al. 2002, Polehampton et al. 2002). A deuterium abundance of D/H $\sim$ 0.2-11 10^{-6} has been derived for molecular clouds in agreement with other determinations in the Solar neighbourhood. The hydrogen fluoride HF has been discovered through its $J = 2-1$ band at 121.7 μm (Neufeld et al. 1997). HF is the dominant reservoir of gas-phase fluorine and, assuming that the absorption arises in the warm envelope, the derived abundance ($\sim 3 \times 10^{-10}$) indicates a strong depletion of fluorine onto dust grains. However, Ceccarelli et al. (2002) mentioned that this absorption could also be due to the hot absorbing layer, in which case the abundance would be an order of magnitude larger. This illustrates that the interpretation of such data is not straightforward, since several components with different physical properties can participate to the detected absorption, as exemplified in the work of Vastel et al. (2002) for the C^+ and O^0 fine-structure lines.

Original results have also been obtained on hydrocarbons and carbon chains. Cernicharo et al. (2002) have found a new line at 57.5 μm which may be the first detection of C_4 (another possible carrier is C_4H). The required abundance of C_4 would make it the most abundant carbon chain in interstellar and circumstellar media. Other polar carbon chains such as cyanopolynes ($HC_{2n+1}N$ with $n = 1-5$) were already detected in the millimeter, but ISO has allowed the detection of pure carbon chains through their low-energy bending modes which fall in spectral regions totally absorbed by the Earth's atmosphere. On the other hand, ro-vibrational emission lines of HCN and C_2H_2 have been found in warm (a few 100 K) molecular cores with abundances $\sim 10^{-7}$ and a likely scenario is that these lines are pumped by warm dust IR emission (Boonman et al. 2003). The methyl radical CH_3 has been discovered in absorption toward Sgr A* with SWS through its ν_2 Q-branch at 16.5 μm and the $R(0)$ line at 16.0 μm (Feuchtgruber et al. 2000). The relatively high abundance of CH_3 ($\sim 10^{-8}$) together with the low abundances of other hydrocarbon molecules (CH, CH_4 and C_2H_2) is inconsistent with the results of published pure gas-phase models of dense clouds. The authors suggest that models including diffuse and translucent clouds or translucent clouds with gas-grain chemistry may resolve this discrepancy.

2.2. The coupling between gas and dust in low-excitation PDRs

PDRs (Photon-Dominated Regions) are ubiquitous in the Galaxy since any interstellar cloud exposed to the ambient radiation field will develop such an interface. More generally, PDRs dominate the IR emission of galaxies and are used to trace their star formation activity (e.g., Förster–Schreiber et al. 2004). Early observations of bright, highly excited PDRs (e.g., Harper et al. 1976, Melnick et al. 1979) have led to detailed modelling where the thermal and chemical balance of the gas is fully described. Physical conditions (radiation field intensity and gas density, see below) in PDRs were then obtained from the comparison between model predictions and observations (see the review in Hollenbach & Tielens 1999). These studies have pointed out the importance of gas-dust interactions and the need to study them further. Among these interactions, the most important are the photoelectric effect on dust which heats the gas and the formation of the H_2 molecule on the surface of grains which triggers the chemistry[1]. The gas state thus results from a balance between photon-driven processes (photoelectric effect on dust, photodissociation of H_2,...) and density dependent reactions (electron recombination, H_2 formation on grains,...). Hence, the excitation of PDRs is usually described with χ, a scaling factor for the intensity of the radiation field in the FUV[2], and with the local gas proton density $n_{\rm H}$. Observations - including the ISO mission - have been primarily performed on nearby PDRs which can be spatially resolved. Among these regions, those with an edge-on geometry represent ideal targets for the study of gas-grain interactions, dust evolution and chemical stratification as a function of depth (or UV field intensity) within the cloud.

PDRs have been extensively observed with the four instruments of ISO, spanning a wide range of physical conditions. Thanks to the sensitivity of the ISO instruments, the sample of observed PDRs has been extended towards low-excitation regimes ($\chi \lesssim$ a few 1000 and $n_{\rm H} \lesssim 10^4$ cm^{-3}) allowing a detailed study of important microscopical processes. In low-excitation PDRs, the gas thermal budget is amenable to a few dominant processes (Kemper et al. 1999, Habart et al. 2001): the heating is due to the photoelectric effect on dust and the cooling occurs through the fine-structure line emission of C^+ (158 μm) and

[1] Gas-grain and gain-grain collisions are also important. These processes, however, primarily affect the dust (size distribution, structure and composition) and they are discussed in Section 3.4.

[2] For $\chi = 1$ the stellar intensity is $4\pi\nu I_\nu = 1.2\,10^{-6}$ W/m^2 at $\lambda \sim 100$ nm, i.e. the average interstellar value in the solar neighbourhood (Mathis et al. 1983).

O^0 (63 and 145 μm). These lines, measured by ISO-LWS, have been used to derive the efficiency of the photoelectric heating, assuming thermal balance (heating = cooling). This efficiency, noted ϵ, represents the fraction of the stellar energy absorbed by a given dust population that goes into gas heating. In practice, ϵ can be determined observationally by correlating the gas cooling line to the dust emission. In such a detailed study towards L1721, an isolated cloud heated by a single B-star ($\chi \sim 4$ and $n_{\rm H} \sim 3000\,{\rm cm}^{-3}$), Habart et al. (2001) have shown that the photoelectric heating is dominated by the smallest grains (of radii $\lesssim 1$ nm and called PAHs, see Section 3) with $\epsilon_{\rm PAH} \sim 3$ %. These results have confirmed the theoretical treatment of the gas photoelectric heating (Bakes & Tielens 1994, Weingartner & Draine 2001a) used in current PDR models. Towards high-latitude, diffuse clouds ($\chi \sim 1$ and $n_{\rm H} \sim 100\,{\rm cm}^{-3}$), Ingalls et al. (2002) have found a statistical correlation between the C^+ line and the far-IR emission of big grains (radii $\gtrsim 10$ nm) as measured with IRAS at 60 and 100 μm which corresponds to an efficiency of $\sim$4.3 %. This latter value, about 1.5 times larger than the theoretical predictions of Weingartner & Draine (2001a), suggests that small grains (PAHs and VSGs, see Section 3.1) undergoing temperature fluctuations contribute significantly to the IR emission.

Other studies made use of PDR models treating in detail the gas thermal balance to analyse observed cooling lines. The [C^+] 158 μm and [O^0] 63 μm dominant lines were successfully explained with the current treatment of photoelectric heating (Timmermann et al. 1998, Kemper et al. 1999, Liseau et al. 1999, Habart et al. 2001 and 2003, Li et al. 2002, Okada et al. 2003, Schneider et al. 2003) confirming independently the photoelectric heating rate used in models. These studies have also shown that the major cooling lines are optically thick, even in low-density PDRs ($n_{\rm H} \lesssim 10^3\,{\rm cm}^{-3}$). In particular, the source geometry and line transfer proved to be important for the O^0 transitions (Li et al. 2002, Okada et al. 2003). In most cases, the O^0 emission line ratio 63 μm/145 μm cannot be readily explained (Liseau et al. 1999) and recent work (Mizutani et al. 2004) has suggested absorption in the [C^+] 158 μm and [O^0] 63 μm lines and/or a quenched photoelectric heating as the possible cause of this discrepancy. Finally, comparison of spatial profiles of the C^+ and O^0 lines to model results has shown that the abundance of PAHs is strongly depressed (by up to a factor 5) in shielded regions (Habart et al. 2001 and 2003). A comparable result has been found in the diffuse medium, traced by the emission of small grains as seen by CAM (Section 3.4).

More indirect analysis of PDRs has also been conducted using the [O^0] 63 and 145 μm and [C^+] 158 μm gas cooling lines detected in absorption and/or emission with LWS towards the Galatic centre, in

Sgr B2 (Vastel et al. 2002, Goicoechea et al. 2004). These observations have allowed to disentangle the contribution of the three layers (C^+/C^+-C^0/CO) predicted by PDR models. The lines intensities of the three lines indicate that $\chi \sim 10^3 - 10^4$ and $n_{\rm H} \sim 10^3 - 10^4\,{\rm cm}^{-3}$ in the PDRs (Goicoechea et al. 2004). The [C^+] 158 μm line is seen in absorption, confirming that this main cooling line of the ISM can be optically thick. Moreover, Vastel et al. (2002) show that atomic oxygen is associated with the three layers. Less than 30% of the total O^0 column density ($\sim 3 \times 10^{19}\,{\rm cm}^{-2}$) comes from the external (C^+) layers. On the other hand, $\sim$ 70% of gaseous oxygen is in the atomic form and not locked up in CO in the molecular clouds lying along the line of sight. This latter result is not explained by current PDR models. This may be related to the low H_2O abundance detected by the SWAS satellite and which is not explained by current chemical networks (Roberts & Herbst 2002). More observations of O^0, O_2 and H_2O in molecular clouds are necessary to solve this issue.

For the first time, the pure rotational bands of H_2 have been detected with SWS towards many PDRs providing a direct probe of the gas temperature. In low-excitation PDRs, current PDR models failed to account for this emission, suggesting an enhanced H_2 formation rate. Observations also suggest that small grains (radii $\lesssim$ 10 nm) play an important role in the formation mechanism. This issue is discussed in the review on molecular hydrogen by Habart et al. (this volume).

2.3. Non-thermal gas motions

Non-thermal motions can play an important role in exciting and mixing the interstellar gas. Some of the underlying processes are directly related to stars (outflows, winds) and are discussed elsewhere in this volume (Nisini et al., Peeters et al.). We discuss here processes that pervade most of the ISM, namely, motions resulting from magneto-hydrodynamical (MHD) turbulence and motions driven by the ambient radiation field.

MHD turbulence has been studied by Falgarone et al. (1999, 2004) from SWS observations of the pure rotational lines of H_2 in emission along a deep sightline in the Galactic plane, sampling the cold diffuse ISM (i.e., avoiding star forming region and molecular clouds). The detected H_2 excitation has shown the presence of a small fraction (a few percents) of warm gas (a few 100 K). This confirms more directly earlier absorption measurements of molecules (CH^+, OH, HCO^+) that can only form in warm gas through endothermic reactions. As illustrated in Figure 1, collisional excitation by MHD turbulence (in shocks or vortices) can successfully account for the excited H_2. In addition, the

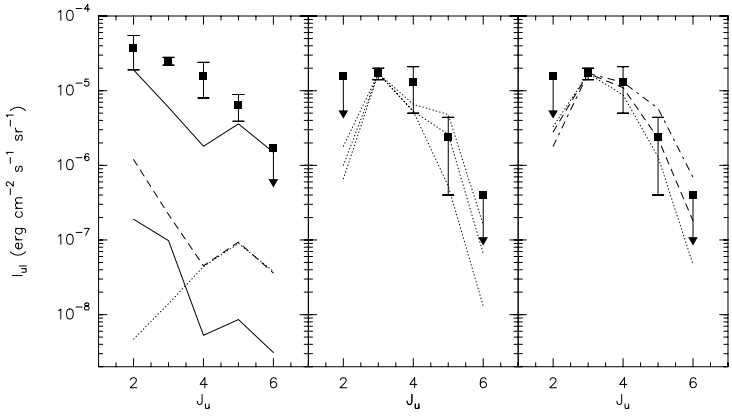

Figure 1. SWS Intensities (solid squares) of the pure H_2 rotational lines in the cold diffuse medium. J_u is the upper rotational number of the transition. **Left:** The contribution of background PDRs on the line of sight (upper solid line) consists of: (1) 19 diffuse PDRs in the Solar neighbourhood ($\chi = 1$, $n_{\rm H} = 30\,{\rm cm}^{-3}$ and $A_{\rm V} = 0.3$, lower solid line), (2) 5 diffuse PDRs in the molecular ring ($\chi = 10$, $n_{\rm H} = 100$ ${\rm cm}^{-3}$ and $A_{\rm V} = 2$, dashed line) and (3) 7 dense PDRs in the molecular ring ($\chi = 10$, $n_{\rm H} = 10^4\,{\rm cm}^{-3}$ and $A_{\rm V} = 2$, dotted line). The fluorescence contribution of low-density PDRs is too low to account for the fluxes of the excited H_2 rotational lines. **Centre:** Residual H_2 line intensities once the PDR-type emission (see left panel) has been removed (solid squares). Models of H_2 lines emission from a few tens of MHD shocks (dotted lines) at 8 (lower), 10 and $12\,{\rm km\,s}^{-1}$ (upper). **Right:** Same residuals compared to the emission of about 10^4 magnetized coherent vortices of rotational velocity $4\,{\rm km\,s}^{-1}$(dot-dashed) and $3.5\,{\rm km\,s}^{-1}$(dashed). The dotted line releases the assumption of statistical balance of the H_2 level populations. Taken from Falgarone et al. (2004).

required number of turbulent structures can also explain the observed CH^+ abundances. More recent studies with FUSE towards stars in the Solar neighbourhood find similar fractions of warm gas (Gry et al. 2002). This suggests that turbulent motions occur with similar rates throughout the inner parts of the Galaxy. In the near future, the spectrometer of the Spitzer Space Telescope will look at the H_2 excitation towards a wider variety of Galactic sightlines as well as in other galaxies. Turbulent motions have also been traced indirectly in cirrus clouds through their impact on the dust size distribution (Section 3.4).

In the warmer environment of PDRs, non-thermal motions are dwarfed by thermal processes and their signature is more allusive. For instance, a possible explanation of the low ortho-to-para ratio of H_2 observed in the warm layers (a few 100 K) of several PDRs are advection mo-

tions due to the propagation of photodissociation fronts (Habart et al., this volume). However, a quantitative estimate of the efficiency of this process awaits a dedicated modelling effort.

3. The nature and evolution of interstellar dust grains

Observations of IR features in emission or absorption provide important constraints on the nature, composition and properties (size distribution, structure) of the dust particles. Work prior to the ISO mission (e.g., Sellgren 1984, Désert et al. 1990, Dwek et al. 1997) has shown that interstellar dust comprises a population of small grains (radii $a \lesssim$ 10 nm) that absorbs about half the energy radiated away by stars and reemit this energy during temperature fluctuations. As discussed in Section 2.2, small grains play an important role in the physics and chemistry of the interstellar gas. These small grains are believed to be predominantly carbonaceous (e.g., Draine 2003) and we will discuss their size in terms of the number of carbon atoms they contain, $N_{\rm C}$. The smallest of them ($a \lesssim 1$ nm and $N_{\rm C} \lesssim$ a few 100) are the carriers of a family of IR emission bands between 3 and 13 μm characteristic of aromatic rings (Duley & Williams 1981) and we call these features the *aromatic IR bands* (AIBs). To explain these bands, a family of large aromatic molecules, the *Polycyclic Aromatic Hydrocarbons* or PAHs has been proposed (Léger & Puget 1984, Allamandola et al. 1985). As discussed below (Sections 3.1 & 3.2), the PAH model explains the main properties of the AIB observations, but still lacks a precise spectroscopic identification with terrestrial analogues. Dust emission at mid-IR wavelengths (e.g., in the IRAS 25 and 60 μm bands) has been ascribed to somewhat larger carbonaceous grains ($1 \lesssim a \lesssim 10$ nm) called *Very Small Grains* or VSGs (Désert et al. 1990). Finally, the far-IR dust emission ($\lambda \gtrsim 30$ μm) is ascribed to a mixture of large graphite and silicated grains or *big grains* ($a \sim$ a few 10 to a few 100 nm, e.g., Li & Draine 2001, Weingartner & Draine 2001b) which emit while being in thermal equilibrium with the radiation field.

The ISO instruments have measured the IR emission of dust particles of all sizes in a wide variety of astrophysical environments. The analysis, still ongoing, of this large database has already lead to important steps forward in our understanding of interstellar dust as exemplified here and in other reviews of this volume. ISO observations of the mid-IR dust emission spectrum have highlighted the properties of PAHs and VSGs as well as their evolution in the interstellar lifecycle. For the first time, direct evidence of important variations of the abundance of small grains in diffuse and cold clouds has been found in deep

photometric ISO data. These latter results point at the importance of dust processing in the interstellar medium (see Section 3.4).

3.1. The emission spectrum of small grains and its implications

One of the prominent results of ISO was to show the ubiquitous presence of the AIBs (at 3.3, 6.2, 7.7, 8.6, 11.3 and 12.7 μm, see Figure 2) in the interstellar medium of the Galaxy (e.g., HII regions: Peeters et al. 2002; planetary nebulae: van Diedenhoven et al. 2004, Uchida et al. 2000; PDRs: Cesarsky et al. 2000b, Verstraete et al. 2001, cirrus and diffuse ISM: Boulanger et al. 1996, Mattila et al. 1996, Chan et al. 2001, Kahanpää et al. 2003) but also in external galaxies (see the reviews by Sauvage et al. and Verma et al. in this volume). Furthermore, the ratio of the 7.7 μm band to the local continuum has now become a tool to measure the starburst activity in galaxies (Lutz et al. 1998).

In the cool ISM, away from hot stars (of spectral type earlier than B2), the 6-13 μm AIB spectrum has been found to be strikingly similar considering the large range of excitation conditions spanned by the observations ($\chi \sim 1$ to 10^4, Boulanger et al. 2000, Uchida et al. 2000, Chan et al. 2001, Verstraete et al. 2001). Conversely, the AIB spectrum towards compact HII regions and circumstellar environments changes significantly as shown in Hony et al. (2001), Peeters et al. (2002) and van Diedenhoven et al. (2004). The authors argued that these variations are due to composition changes in a population of PAHs including substituted and metal complexed species. In fact, newly formed PAHs are expected to be found in the ejecta of evolved stars while in the general interstellar medium (which includes the cool ISM), the population of PAHs has already been processed by the ambient UV radiation field and shocks over long timescales ($\sim 10^8$ yrs). In the following we call the AIBs observed in the interstellar medium, the IS-AIBs (interstellar AIBs). We discuss below the IS-AIBs while the AIBs around stars and HII regions are discussed in Peeters et al. (this volume).

For the first time, most AIBs were spectrally resolved by the ISO spectrometers. Individual AIBs have been found to be broad (λ/FWHM $\sim$ 30 to 80), smooth and in some cases clearly asymmetrical (the 3.3, 6.2 and 11.3 μm bands all show a prominent red wing). As shown in Boulanger et al. (1998b) and Verstraete et al. (2001) the AIBs are well represented with Lorentzian profiles possibly indicating that the AIB carriers are large molecules. Other methods of decomposition have been applied to quantify the AIB intensities (Peeters et al. 2002, Uchida et al. 2000) illustrating the importance of the AIB definition for the extraction of the underlying continuum. SWS data has

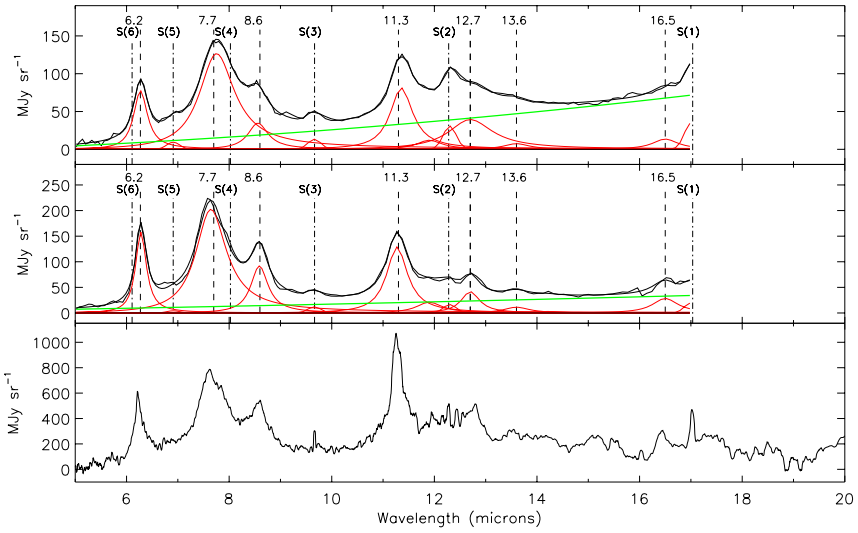

Figure 2. Typical CAM (spectral resolution R ∼40, top and middle panels) and SWS (R ∼ 200, bottom panel, from Verstraete et al. 2001) spectra in NGC 2023 (from Abergel et al. 2002). For the CAM spectra, the aromatic lines are fitted with Lorentzian profiles, while the S(1), S(2) and S(3) pure rotational lines of H_2 are adjusted with gaussian profiles. The continuum arises further inside the molecular cloud than the AIBs (top panel).

clearly shown that the 7.7 μm-feature consists of several components (Joblin et al. 2000, Peeters et al. 2002), including the two main features at $\sim$ 7.6 and 7.8 μm first reported by Bregman (1989). New features have been added to the PAH family, like the 16.4 μm band (van Kerckhoven et al. 2000, Moutou et al. 2000). This band has been assigned by the latter authors to PAHs containing pentagonal rings, species which are important in chemical networks of PAH and soot formation (Moutou et al. 2000). The 16.4 μm band is also present in CAM-CVF data but falls at the detection edge of the detectors (Figure 2). Some AIBs have also been detected in absorption (see Section 3.3). More recently an emission band at 4.65 μm has been assigned to deuterated PAHs (Peeters et al. 2004). More features are expected to be found in the ISO archive but also thanks to the Infrared Spectrograph (IRS) now operating on the Spitzer Space Telescope. A recent study on the PDR NGC 7023 reports new features at 6.7, 10.1, 15.8, 17.4 and 19.0 μm (Werner et al. 2004). Features in the far-IR and submm range could also be detected in the future by the Herschel Space Observatory (Joblin et al. 2002).

In the IS-AIB spectrum, the positions and widths of the major bands (3.3, 6.2, 8.6 and 11.3 μm) are stable (within a few cm^{-1}, Verstraete et al. 2001), conversely to spectra towards HII regions and circumstellar environments where significant shifts of the 6-9 μm bands are observed (Peeters et al. 2002). To constrain the nature of PAHs, detailed comparisons between the observed AIBs and the laboratory and theoretical data on small ($N_C \leq 50$), planar, aromatic molecules have been carried out. Pech et al. (2002) have shown that the profiles of the 6.2 and 11.3 μm bands observed in the planetary nebula IRAS 21282+5050 can be explained with the emission of a mixture a medium-sized PAHs ($30 < N_C < 80$) having similar spectroscopic properties. The band positions and widths arise then naturally from the molecular anharmonicity during temperature fluctuations (see Section 3.2). Thus, the strong variability of the vibrational spectrum of terrestrial PAHs as a function of charge state, hydrogen coverage and chemical structure (e.g., Hudgins et al. 2000, Pauzat et al. 1997, Langhoff 1996) is not reflected in the IS-AIBs of the cool ISM where PAHs are expected to be for instance neutral ($\chi \sim 1$ to a few 100) or ionized ($\chi \sim$ a few 10^3, Dartois & d'Hendecourt 1997). Furthermore, a precise, quantitative assignation of major AIBs is still not achieved: the components of the 7.7 μm and the 8.6 μm bands are not explained by the properties of small terrestrial PAHs (Verstraete et al. 2001, Peeters et al. 2002). Spectroscopic evidence (van Kerckhoven et al. 2000, Hony et al. 2001) and modelling (Schutte et al. 1993, Li & Draine 2002) has pointed out the importance of large PAHs ($N_C \geq 50$) for the 6-13 μm AIBs. The vibrational bands of such large systems may be less sensitive to the structure, shape, charge and surface state and provide a better understanding of the observed AIBs. However, recent calculations by Bauschlicher (2002) on the large PAH $C_{96}H_{24}$ seem to challenge this picture while laboratory measurements on large systems are still awaited.

Another conspicuous aspect of the mid-IR spectrum of the ISM is the presence of broad features (λ/FWHM $\sim$ 10) and continua underneath the AIBs. These spectral components are seen in the very excited environments studied by Peeters et al. (2002) such as planetary nebulae but also in the cool ISM (see Figure 2). The intensity of the broad features around $\sim$ 7, 10 and 12 μm are best delineated in SWS data where all AIBs are spectrally resolved. Their detailed shape however is poorly constrained (Verstraete et al. 2001). This emission has been discussed in the past and proposed to be associated to the AIB spectrum but

not directly correlated with the bands[3] (Cohen et al. 1985, 1986, 1989; Roche et al. 1989; Bregman 1989). These broad features and continua may arise from larger species ($N_C \gtrsim$ a few 100) as suggested by several CAM studies of the spatial distribution of this broad-band emission relative to the AIBs in PDRs (Section 3.4). Here also laboratory and/or theoretical spectroscopy of carbon clusters is needed to quantitatively interpret these broad bands and continua.

3.2. Emission mechanism of the aromatic infrared bands and modelling

The high sensitivity and dynamical range of the ISO instruments has provided detection of the AIBs from diffuse to bright regions. In particular, it has been found that the integrated flux of the AIBs globally scales with the intensity of the FUV radiation field as long as $\chi \leq 10^4$ (Boulanger et al. 1998a, Uchida et al. 2000). This strongly supports a picture in which small grains are transiently heated to high temperature each time they absorb a UV photon (Puget et al. 1985, Sellgren et al. 1985). It has also been shown that the AIBs can be excited by visible photons (Uchida et al. 1998) and this is well explained by AIB emission models, provided that PAHs are ionized or large (Li & Draine 2002). Studies of the visible, near-IR absorption cross-sections of PAHs with different sizes and in different charge and hydrogenation states are important, since, for instance, in the standard galactic radiation field (Mathis et al. 1983), PAHs absorb about half of their energy in this wavelength range.

On the other hand, the high spectral resolution of the SWS has stimulated much work on the AIB profiles and on their formation mechanism. Indeed, this dedicated spectroscopy has provided a unique opportunity to compare to laboratory results. Specifically, detailed studies of the IR emission spectra from small, gas-phase PAHs excited by UV photons or thermally heated, have shown that the spectral profile (position and width) of the bands depends on the internal vibrational energy (or temperature) of the molecule (Kim et al. 2001, Cook et al. 1998 and references therein, Joblin et al. 1995). The observed emission profiles hence result from the sum of the individual lorentzian profiles formed during the cooling of the molecule after UV excitation. The asymmetrical profiles of the 3.3, 6.2 and 11.2 μm bands can thus be explained with an intramolecular broadening due to coupling between vibrational modes in PAHs (Pech et al. 2002). Assuming similar spectroscopic properties for a broad range of PAH size, the stability of the 6-13 μm IS-AIBs

[3] The laboratory spectra of individual PAH molecules do not seem to present any continuum (e.g., Joblin et al. 1995).

is naturally explained by an emission during thermal fluctuations which span a large range of temperatures. In this framework and from detailed profile modelling, one can also infer a photodissociation threshold (in terms of internal energy per carbon atom, a few 0.1 eV/C) beyond which small PAHs are destroyed. The smallest PAHs ($N_{\rm C} \lesssim 40$) carrying the 3.3 μm band would then be "selected" by photodissociation leading to similar distribution of internal energy. This would explain why the profile of this AIB is so stable in increasingly excited PDRs (Verstraete et al. 2001, van Diedenhhoven et al. 2004).

Finally, the mid-IR spectra observed by the ISO has allowed an empirical definition of the size-dependent IR cross-sections of PAHs and VSGs which have been used in recent quantitative modelling of the dust emission (Li & Draine 2001).

3.3. Mid-infrared extinction

The extinction curve is one of the main tool to study interstellar dust, to correct the photometry of embedded sources and to convert the measured extinctions into column densities. Before ISO, the mid-IR extinction curve was thought to be relatively well understood, and described with a power law $A_\lambda \sim \lambda^{-1.7}$ from $\sim 1\,\mu$m down to a pronounced minimum around 7 μm due to the increasing contribution of the silicate absorption feature at $9.7\,\mu$m. It was explained by the absorption of a mixture of graphite and silicate grains (Draine 1989). The situation is now more controversial, as illustrated in the Figure 4 of the recent review of Draine (2003). Using the measurements of hydrogen recombination lines with the SWS, Lutz et al. (1996) and Lutz (1999) have shown that the IR extinction towards Sgr A* does not decrease with increasing wavelengths from 4 to 8 μm, and as a consequence does not present any minimum near $7\,\mu$m. On the other hand, Rosenthal et al. (2000), using rovibrational lines of H_2 detected by the SWS in Orion, have found that the mid-IR extinction decreases with increasing wavelengths and presents a minimum at $\sim 6.5\,\mu$m, as expected. The IR extinction curve depends on the composition of dust grains and to a lesser extent on their size distribution (for $\lambda \lesssim 2$ μm) and may vary from place to place. New observations are therefore necessary to clarify this controversy.

The IR extinction curve also presents a number of faint features detected with the SWS towards the Galactic centre and other sources with large extinction (Schutte et al. 1998, Chiar et al. 2000, Chiar & Tielens 2001, Bregman & Temi 2001). The ubiquitous $3.4\,\mu$m band is generally attributed to CH stretching in aliphatic hydrocarbons. The asymmetrical deformation modes of CH at $\sim 6.9\,\mu$m have been detected

before ISO with the KAO (Tielens et al. 1996), but the symmetrical deformation mode at 7.2 μm has been found for the first time by Chiar et al. (2000) with SWS data. The strengths of the 3.4, 6.9 and 7.2 μm features appear compatible with the hypothesis that Hydrogenated Aliphatic Carbon (HAC) is the main carrier. Finally, the 3.3 and 6.2 μm bands are detected in absorption towards several lines of sight, and are attributed to C–H and C–C stretching modes in aromatic hydrocarbons, respectively. However, as mentionned by Chiar & Tielens 2001, the 6.2 μm band is not detected in the diffuse medium, which suggest that this absorption band is circumstellar in nature. At this time the absorption of other aromatic bands have not been evidenced in the SWS data. As mentioned by Bregman & Temi (2001), a calibration problem in the SWS data at 11.1 μm may preclude the detection of the 11.2 μm band in absorption. These authors have discovered an absorption band centered at 11.2 μm from ground-based spectra of the molecular cloud surrounding Monoceros R2 IRS 3, and attributed this band to the C-H out-of-plane vibrational mode of PAHs.

3.4. Dust evolution and processing

The dense shells around evolved stars are known to form dust grains as demonstrated by observations of the dust IR emission and absorption features in these objects (e.g., Blommaert et al., Molster & Kemper and Peeters et al. in this volume). The timescale of this stardust injection is $\sim 10^9$ yrs. On the other hand, theoretical studies show that dust grains are efficiently destroyed in supernova shocks (Jones et al. 1994) with a lifetime $\sim 10^8$ yrs. Efficient mechanisms for grain growth must therefore exist in the other phases of the interstellar medium, most probably in dense, cold clouds where the rates of grain coagulation and accretion of gas phase species are expected to be the largest.

High energy gas-grain collisions lead to erosion by vaporization (sputtering), while low energy collisions lead to the reverse process of gas accretion onto dust (Jones et al. 1994). Collisions between large grains (radii $\gtrsim$ 100 nm) at velocities above a few km/s lead to fragmentation into small grains (radii $\lesssim$ 1 nm) or even grain destruction. By contrast, coagulation occurs through low energy collisons (Jones et al. 1996). UV irradiation can also play a major role by destroying dust grains in high excitation regions (with typically $\chi > 10^4$) and also photo-evaporating condensed species. Evidence for photoprocessing of PAHs and VSGs has been found towards HII regions where the 6-13 μm emission spectrum is dramatically different from the IS-AIBs (Roelfsema et al. 1996, Verstraete et al. 1996). Such processing must leave specific signatures in the dust size distribution and optical properties which in turn affect

the gas thermal state and chemistry. As we discuss below, ISO has brought important observational evidences of the evolution of the dust size distribution in the ISM, from diffuse cirrus clouds to dense cores.

PDRs: Grain dynamics driven by the radiation field could play a major role in the observed evolution of the mid-infrared spectrum across PDRs. Size segregation in regions anisotropically irradiated by stars may arise from radiation pressure and recoil forces (due to the photo-ejection of electrons, the photodesorption of weakly-bound surface species and the formation of molecular hydrogen, see Weingartner & Draine 2001c). This process could strongly modify the size distribution at the illuminated surface of PDRs. Furthermore, the gas in PDRs is suddenly heated and ionized, and experiences a strong pressure gradient. It flows supersonically from the molecular cloud surface to the tenuous intercloud medium, carrying away dust grains. In this highly turbulent flow, grain-grain collision might be strong enough to fragment big grains. This process could explain spectro-imaging observations with CAM across several low-excitation PDRs (NGC 2023, NGC 2068, NGC 2071, NGC 7023, ρ Oph, see Abergel et al. 2002 and 2003b, Rapacioli et al. 2004) showing that the ratio of the AIBs (especially around 7.7 μm) to the underlying continuum is higher in the photodissociated interface than in more shielded regions.

Variations related to a transition in the charge state of PAHs are also expected. Indeed, PAHs are predicted to be neutral inside dense clouds, and positively ionised in the low-density regions facing the illuminated surface of PDRs (e.g., Dartois & d'Hendecourt 1997). Laboratory data and theoretical calculations show that the single ionization of PAHs strongly enhances (by a factor of $\sim$ 10) the emissivity of the C-C stretching (6.2 and 7.7 μm) and the C-H in plane bending (8.6 μm) modes, with respect to the intensity of the C-H out-of-plane bending features at 11.3 and 12.7 μm (Hudgins et al. 2000, Langhoff 1996, Szczepanski & Vala 1993). Yet, as already discussed in Section 3.1 a direct decomposition of the mid-IR dust emission spectrum shows only limited variations of the AIB ratios in the cool ISM (factor 2 or less, e.g. Uchida et al. 2000). Rapacioli et al. (2004) went one step further by applying the singular value decomposition method to CAM-CVF data in order to extract typical emission spectra for the different population of small grains in PDRs. Three elementary spectra could be extracted (Figure 3):

- The first two spectra are dominated by the AIBs and attributed to neutral PAH and PAH cations. The differences between these two spectra follow the expected changes due to ionisation (increase of the (6.2-7.7-8.6 μm)/(11.3-12.7 μm) band ratio and blueshift of the 11.3 μm

band in cations according to Hudgins & Allamandola (1999). The PAH cation spectrum is dominant in the low-density gas surrounding the star whereas the PAH neutral spectrum dominates at the interface with the molecular cloud.
- The third spectrum contains a strong continuum and dominates behind the illuminated edge of the PDR (far from the illuminating star), and is attributed to very small carbonaceous grains. The fact that a similar spectrum has been seen on a few pixels of the CAM map of the illuminated edge of Ced 201 (Cesarsky et al. 2000a) lends confidence to the analysis performed by Rapacioli et al. (2004). Several features visible in the spectrum indicate a possible aromatic nature of the carriers. Interestingly, the 7.8 μm component of the broad 7.7 μm feature appears to be carried by this population. The authors also argued that these carbonaceous VSGs could be the progenitors of free PAHs. Indeed, the drop of the VSG emission at the cloud edge appears to be correlated with the increase of the neutral PAH emission. These VSGs may be clusters of PAHs which photoevaporate at the surface of clouds. This idea is consistent with the strong spatial variations observed in the IRAS 12/100 μm ratio at the surface of molecular clouds (Boulanger et al. 1990, Bernard et al. 1993). The Spitzer Space Telescope observations are underway to confirm these results on a larger sample of objects (the CAM-CVF data suffer from stray light artefacts which limit their useful dynamics, see Boulanger et al. 2004), and search for new features at longer wavelengths which can be attributed to these VSGs.

It should be emphasized that the question of the formation of PAHs in the ISM is still open. Some PAHs could be formed in the outflows of evolved carbon-rich stars in a chemical kinetic scheme based on soot formation in hydrocarbon flames (Frenklach & Feigelson 1989, Cherchneff et al. 1992). Cernicharo et al. (2001) detected C_4H_2, C_6H_2 and C_6H_6 towards the proto-planetary nebula CRL 618, showing that aromatic molecules can indeed be formed in such objects and that energetic processes such as UV irradiation or shocks play an important role in the chemistry of these species.

Cirrus Clouds: Important variations of the PAH abundance have been observed in diffuse regions like cirrus clouds. Based on a comparison between CAM-LW2 (6.7 μm broad band) and radio data, Miville-Deschênes et al. (2002) have shown variations of the abundance of PAHs by up to a factor 10 in a high latitude cirrus cloud. High PAH abundances were found in regions with strong turbulent motions, while low abundances were associated with regions of shallower turbulent motions where CO emission is also detected (see Figure 4). This study highlights

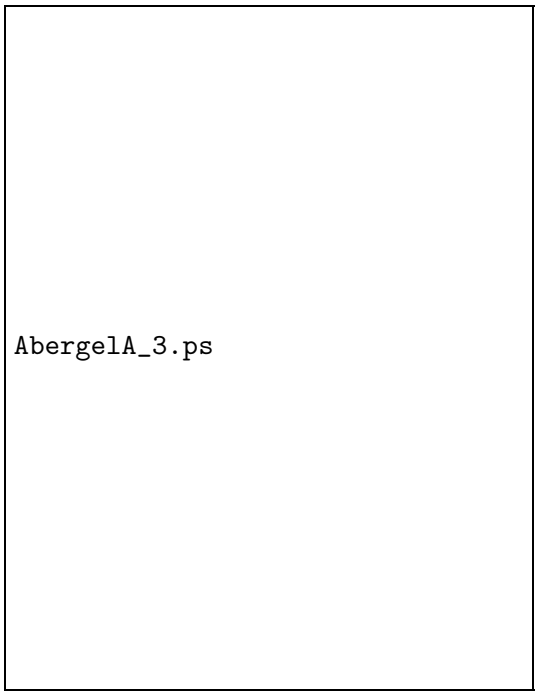

Figure 3. Elementary spectra extracted from spectro-imaging CAM observations of NGC 7023 (Rapacioli et al. 2004). These spectra are attributed to PAH cations (upper panel), neutral PAHs (middel panel) and very small carbonaceous grains (lower panel).

for the first time the important role of the gas turbulent motions on the evolution of the grain size distribution. The depletion of small grains observed in the denser parts of cirrus clouds is the first step of the dust coagulation seen in cold clouds.

Cold Clouds: Depletion of PAHs and VSGs in the dense regions of molecular clouds has also been shown by ISO data, suggesting the importance of dust coagulation processes in the ISM. IRAS images first showed that the emission from small grains at 12, 25 and 60 μm, relative to that from big grains (in thermal equilibrium with the radiation field) at 100 μm, varies by one order of magnitude among and within translucent clouds in the nearby ISM (Boulanger et al. 1990). Standard model calculations predict that the FIR emission of dust in thermal equilibrium with the radiation field follows a modified black body with a spectral index β between 1 and 2 (e.g., Hildebrandt 1983, Draine & Lee, 1984). The brightness per hydrogen atom can be written: $I_\lambda = \epsilon_{\lambda_0} \times \left(\frac{\lambda}{\lambda_0}\right)^{-\beta} \times B_\lambda(T) = \frac{\tau_\lambda}{N_H} \times B_\lambda(T)$. The dust opacity τ_λ can be derived if the brightness, the column density and the temperature

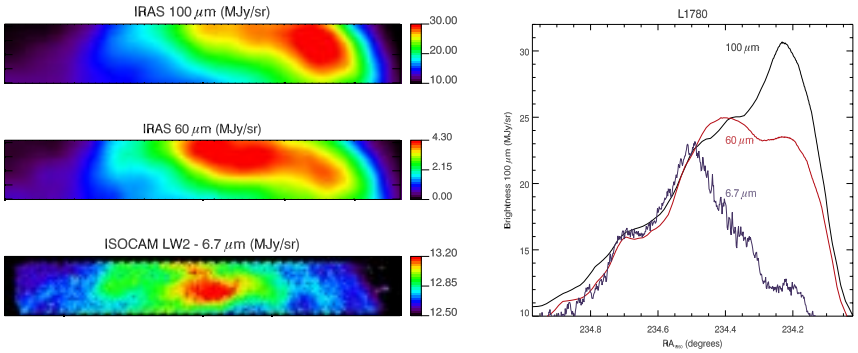

Figure 4. The L1780 cloud (from Miville-Deschênes et al. 2003). **Left:** IRAS 100 μm (top) and 60 μm (middle), and CAM 6.7 μm (bottom) maps across L1780. **Right:** Average emission as a function of right ascension. The 6.7 and 60 μm emissions were scaled to be compared to the 100 μm emission. The spectacular decrease of the 6.7 μm / 100 μm ratio cannot be explained by the attenuation of the radiation field. The abundance of PAHs likely decreases, a trend which is spatially correlated with the apparition of CO emission.

of the emitting particles are known at a given wavelength. However, the main unknown in our understanding of the big dust grains is the FIR emissivity law, due to the observational difficulty to accurately determine the temperature and β independently, together with the column density. FIR observations of a variety of mostly quiescent clouds (i.e. no high mass star formation) have been used to solve this problem.

The longest wavelength that can be measured with PHOT and LWS is slightly more than 200 μm, which is not sufficient to allow an independent determination of β and T. On the other hand, the wavelength coverage of the balloon-borne experiment SPM/PRONAOS ($\lambda = 200$–$580\,\mu$m) is extremely suitable for the determination of β, but PRONAOS is less sensitive to dust temperature (except in the coldest objects, $T < 15$ K, where the spectral energy distribution peaks around the shortest PRONAOS band), so IRAS or PHOT must also be used.

For comparison with dust models, the FIR opacity needs to be gauged against the extinction curve in either the visible or near- infrared. This can be done by determining the optical extinction directly from colour excesses or from star counts. The former method is constrained to a limited amount of sightlines and a maximum extinction. The latter method is also limited to a maximum extinction (of $A_V < 8$), and suffers from higher uncertainties in the denser regions due to a lack of statistical accuracy. A study by Arce & Goodman (1999) showed that for low and moderate density regions ($A_V < 4$), the different extinction estimates are reliable and give similar results. With the advent of large stellar databases (e.g. USNO, 2MASS) it has become much easier to

perform star counts over any area on the sky, providing valuable extinction information. Alternatively, one can estimate the visual extinction from the total gas column density and assuming a ratio A_V/N_{gas}. This indirect method depends on the assumed ratio between gas and dust and the conversion between molecular line strength and column density. Recent observations by FUSE (Rachford et al. 2002) confirmed that ratio between the total hydrogen column density and reddening $N_{H+H_2}/E(B-V)$ is constant up to $E(B-V) \sim 1$ and well described by the constant presented by Bohlin et al. (1978) obtained from the Copernicus satellite data. Very high extinctions can be measured from near-infrared extinction of background emission, first noticed in the ISOCAM images (Perault et al 1996, Abergel et al. 1996) and used to study the very dense cores (Nisini et al., this volume).

For the diffuse ISM associated with atomic hydrogen, Boulanger et al. (1996) found a value of β close to 2.0 and a mean temperature of 17.5 K by correlating COBE data with Dwingeloo HI data. The derived FIR emissivity $\tau(\lambda)/N_H = 1.0\times10^{-25}\ (\lambda/250\,\mu\mathrm{m})^{-2}\,\mathrm{cm}^2$ is close to the value predicted by Draine and Lee (1984) based on a standard dust model. This result suggests that spherical grains are more likely to occur in the diffuse ISM than porous or fractal grains. Assuming $R_V = 3.1$, the result by Boulanger et al. implies $\tau(\lambda)/A_V = 2.9\times10^{-4}(\lambda/200\,\mu\mathrm{m})^{-2}$. We will use this value as a reference in the discussion below. In case of grain processing towards fractal or porous grains, one would expect an increase of the FIR emissivity and a corresponding increase in the value of $\tau(\lambda)/A_V$ (e.g., Ossenkopf & Henning 1994).

The first ISO studies of moderate density regions indicated dust temperatures of 13.5±2 K assuming $\beta = 2$ (Laureijs et al. 1996, Lehtinen et al. 1998). The observed ratios $\tau(200)/A_V$ had large uncertainties but were not inconsistent with the predictions for a standard dust model. For increasing densities (in the range 100 to 10^4 cm^{-3}) the temperature is generally found to decrease from ∼17.5 K to as low as 12 K (Tóth et al. 2000, Juvela et al. 2002, del Burgo et al. 2003, Lehtinen et al. 2004).

The first strong indication that the FIR properties of the dust in moderate density high latitude clouds might deviate from the diffuse ISM was presented by Bernard et al. 1999 based on SPM/PRONAOS and ISO observations of a cirrus cloud in Polaris. Bernard et al. find cold dust at 13.0 K with $\beta = 12.2\pm0.3$. Since the cloud has a low visual extinction ($A_V < 1$), only an anomalously low ambient radiation field could cause such a low temperature, which is ruled out. It was therefore concluded that the dust properties of the large grains have changed in the cloud. The inferred ratio $\tau(200)/A_V = 17 \pm 3\times10^{-4}$ is more than 5 times the value for the diffuse ISM. Other PRONAOS observations

combined with IRAS data of a dense filament in the Taurus molecular cloud by Stepnik et al. 2003 has evidenced temperatures as low as of 12.1 ± 0.2 K in the densest regions (with $\beta = 2$), together with an increase of the FIR emissivity by a factor larger than 3 compared with the diffuse ISM.

Assuming $\beta = 2$, del Burgo et al. 2003 have analysed a sample of moderate density regions ($A_V < 6$) observed with ISO. The regions have dust temperatures in the range from 13.5-15.6 K and one exceptional region with $T = 18.9\,K$. Combination with extinction data from star counts shows that the ratio $\tau(200)/A_V$ is systematically higher than for the diffuse ISM. In fact, a trend was found where $\tau(200)/A_V$ increases with decreasing temperature. A similar trend, although less apparent, was found by Cambrésy et al. (2001) who correlated large scale extinction measurements from starcounts with far-infrared DIRBE data in the Polaris Flare region. They find $\tau(200)/A_V$ in the coldest regions with $T < 15.5$ K to be several times higher than in the diffuse ISM.

Lagache et al. (1998), using COBE data, and Tóth et al. (2000), using ISO serendipity mode data, found that the temperature of the dust can be significantly below 17.5 K over large areas. In these areas, the abundance of small grains is low, as inferred from the absence of 60 μm emission. Earlier studies have revealed a strong anticorrelation between the 60 μm emission and dense gas traced by the millimetre transitions of ^{13}CO (Laureijs et al. 1991, Abergel et al. 1994). In the dense molecular cloud TMC2, a large scale cold component with a uniform temperature of about 12.5 K is evidenced from PHOT data, while only the densest cores show lower temperatures (del Burgo & Laureijs, 2004). The dust spatially associated with the 60 μm emission is significantly warmer ($\sim$19 K with $\beta = 2$). In addition the morphology of this "warm" component is different from the cold component suggesting that the cold and warm components are spatially separate.

The evolution of dust properties with the gas density is believed to be due to the process of gas accretion onto grains and grain coagulation. Gas accretion forms grain mantles typically for $A_V \gtrsim 2$, mainly composed of water ice and carbon oxides (e.g., Teixeira & Emerson, 1999). However, Preibisch et al. (1993) has shown that the presence of such mantles on dust grains does not significantly increase the FIR emissivity. As the gas cools down and condenses, gas turbulent motions become shallow leading to grain-grain collisions with sufficiently low energy to enable grain sticking and coagulation, which can lead to the formation of clusters with an enhancement of the FIR emissivity (e.g., Ossenkopf & Henning 1994, Stepnik 2001, Stepnik et al. 2004) compatible with the PHOT and SPM/PRONAOS observations. Such a scenario can also qualitatively explain the observed trend in the extinction curve,

i.e., an increase in R_V with the density (e.g, Cardelli et al. 1989). At first order, the coagulation process appears to be compatible with the dynamical and cloud evolutionary time-scales. The formation of ice mantles is also believed to increase the sticking probability for coagulation. The physics of grain-grain collisions, coagulation and growth has been studied theoretically (Dominik & Tielens 1997) and in the laboratory (Blum 2004) in the context of proto-planetary disks. However, the efficiency of these processes in the ISM still needs a dedicated modelling taking into account the velocity structure of the ISM (e.g., turbulent and intermittent processes).

In the last decade, laboratory measurements (Agladze et al. 1996, Mennella et al. 1998) have also indicated that, at low temperatures ($T < 30\,K$), the dust optical properties can change significantly, likely because of low-energy structural transformations. A systematic analysis of β from a large compilation of PRONAOS data by Dupac et al (2003) has shown that β is not a constant, but varies with dust temperature: high indices (1.6-2.4) being observed in cold regions (11-20 K) while low indices (0.8-1.6) are observed in warm regions (35-80 K). Although systematic variations in grains size and/or chemical composition as a function temperature cannot be ruled out, the most likely explanation is that the spectral index of dust can change with temperature due to a solid state quantum process. Such studies allow a quantitative understanding of the FIR emission of dust in our Galaxy and in outer galaxies (a cold dust component has also been detected with PHOT in non-active galaxies, see the chapter by Sauvage et al., this volume) and pave the way for the scientific analysis of the Herschel and Planck missions.

4. Structure of the cool ISM

The structure of the ISM strongly affects the chemistry and the star formation activity. Observations of the IR dust emission is unique for tracing interstellar matter over a wide range of physical conditions and, in particular, across the atomic to molecular transition where neither HI nor molecular millimetric lines are robust tracers, because of the local variations of the abundance and the excitation conditions.

CAM broad-band mapping of molecular clouds has shown the spatial distribution of the emission due to small grains with an angular resolution two orders of magnitude better than IRAS at 12 μm. The images are, to first order, anti-correlated with the visible emission (e.g., Figure 5), and contain small scale brightness fluctuations related to illuminated edges of dense regions. For nearby objects with edge-on

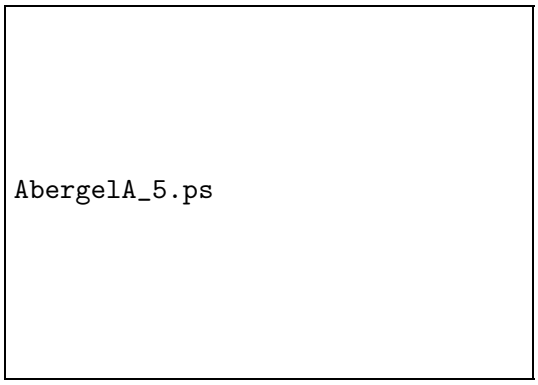

Figure 5. L1630 in the visible (35'×40' field from the UK Schmidt Telescope and extracted from the DSS produced at the STSI) and with CAM (blue: 5-8.5 μm, red: 12-18 μm) from Abergel et al. 2002. The central region (NGC 2023) is saturated because of the dynamic range.

geometry, IR filaments as sharp as $\sim 10''$ (or ~ 0.02 pc at a distance of 400 pc) are detected due to the combined effects of steep density gradients and extinction in the dense regions (e.g., Abergel et al. 2003a in the illuminated edge of the Horsehead nebula). Associated measurements of the penetration length of the incident radiation field gives estimates of the density just behind the illuminated edges. More quantitative constraints on the density profiles can be derived from the comparison of PDR modelling (e.g., Le Bourlot et al. 1993) with spatial profiles of the AIBs as well as of cooling lines or molecular emissions taken with ISO or from the ground (Habart et al. 2001, 2004, Pety et al. 2004). However, caution should be exercised in analysing the spatial profiles observed across PDRs because of the complex interface geometry seen in the high angular resolution data of CAM (e.g., Habart et al. 2004). This is also true of ground-based and of recent Spitzer Space Telescope data.

The spatial structure of the cool ISM appears self-similar in a wide range of scales. With PHOT images of cirrus emission at 90 μm, the power law relation established from IRAS data (Gautier et al. 1992) between the power of the fluctuations and the spatial scale has been extended to twice as high spatial frequencies, while at 170 μm fluctuations at arcmin scales are studied for the first time (Herbstmeier et al. 1998, Kiss et al. 2003). The spectral index is found to vary from field to field ($-5.3 < \alpha < -2.1$), depending on the absolute surface brightness. Higher values of α are found at 170 μm rather than at 90 μm and are attributed to temperature variations of dust. Compared to ISO, the Spitzer Space Telescope has the sensitivity, the angular resolution and

the mapping capabilities to extend significantly these studies (see the first results by Ingalls et al. 2004).

5. Conclusions:

The ISO mission has provided an incredibly rich harvest of gas and dust features in the general interstellar medium away from hot stars, the cool ISM. These results have highlighted the physics and chemistry of interstellar matter and its evolution. Emission and absorption lines of gas phase species were used to constrain the excitation processes (shocks, stellar UV irradiation) of the ISM and represented a major benchmark for the modelling. Similarly, spectroscopy of dust features has allowed a detailed comparison to the properties of terrestrial analogues of interstellar grains. These studies have pointed out the importance of nanometric carbon clusters in space and the need to build a laboratory and/or theoretical database of spectra for a large size range of these species. The spatial distribution of the dust emission observed by the photometers has clearly shown and for the first time, the importance of evolution processes (e.g., photodestruction, grain coagulation) affecting the dust size distribution. The joint observations of dust and gas features have highlighted the gas-grain couplings (photoelectric effect, H_2 formation) and allowed quantitative studies of the underlying microphysics. Furthermore, the quantitative understanding of the gas-to-dust correlation for all dust components is a key issue for the analysis of the extended emission in the future surveys to be conducted with Spitzer, Planck and Herschel, allowing to disentangle brightness fluctuations due to the ISM from those of the cosmic IR and microwave backgrounds.

References

Abergel A., Boulanger F., Mizuno A. et al., 1994, ApJ 423, 59
Abergel A., Bernard J.-P., Boulanger F. et al., 1996, A&A 315, 329
Abergel A., Bernard J. P., Boulanger F. et al., 2002, A&A, 389, 239
Abergel A., Teyssier D., Bernard J. P et al., 2003a, A&A 410, 577
Abergel A., 2003b, in *Exploiting the ISO Data Archive*, Eds. C. Gry, S. Peschke, J. Matagne, P. Garcia-Lario, R. Lorente & A. Salama. ESA SP-511, 177
Agladze N.I., Sievers A.J., Jones S.A., et al., 1996, ApJ 462, 1026.
Allamandola L.J., Tielens A.G.G.M., Barker J.R., 1985, ApJ 290, L25
Arce H.G., Goodman,A.A., 1999, ApJ 517, 264
Bakes E.L.O., Tielens A.G.G.M., 1994, ApJ 427, 822
Bauschlicher C.W., 2002, ApJ 564, 782
Bernard J.P., Boulanger F., Puget J. L., 1993, A&A 277, 609

Bernard J-P., Abergel A., Ristorcelli I., et al., 1999, A&A 347, 640
Blommaert, J., Siebenmorgen, R., Coulais, A. et al. 2003, 'The ISO Handbook, Volume II: CAM - The ISO Camera', ESA SP–1262
Bohlin R.C., Savage B.D., Drake J.F., 1978, ApJ, 224, 132
Boonman A.M.S., van Dishoeck E.F. Lahuis F., 2003, A&A 399, 1047
Boulanger F., Falgarone E., Puget J.-L. et al., 1990, ApJ 364, 136
Boulanger F., Abergel A., Bernard J.-P., et al., 1996, A&A 312, 256.
Boulanger F., Abergel A., Bernard J.-P. et al., 1998a, in *Star Formation with ISO*, eds. J. L. Yun & R. Liseau, Astronomical Society of the Pacific, San Francisco, 15
Boulanger F., Boissel P., Cesarsky D., Ryter C., 1998b, A&A 339, 194
Boulanger F., Abergel A., Cesarsky D. et al., 2000, in *ISO beyond point sources: studies of extended IR emission*, ESA SP-455, R.J. Laureijs, K. Leech & M.F. Kessler Eds.
Boulanger F., Lorente R., Miville-Deschênes M.A. et al., 2004, submitted to A&A
Blum J., 2004, in *Astrophysics of dust*, ASP Conference Series, vol. 309, p.369, A.N.Witt, G.C.Clayton & B.T. Draine Eds.
Bregman J.D., Temi P., 2001, ApJ 554, 126
Bregman J.D., 1989, in *Interstellar dust*, IAU Symp., 135, 109
del Burgo C., Laureijs R. J., Abraham P. & Kiss C., 2003, MNRAS 346, 403
del Burgo C., Laureijs R. J., 2004, submitted to MNRAS
Cambrésy L., Boulanger F., Lagache G., Stepnik B., 2001, A&A 375, 999
Cardelli J., Clayton G.C., Mathis J.S., 1989, ApJ 345, 245
Caux E., Ceccarelli C., Pagani, L. et al., 2002, A&A 383, L9
Ceccarelli C., Baluteau J.-P., Walmsley M. et al., 2002, A&A 383, 603
Cernicharo J., Heras A.M., Tielens A.G.G.M. et al., 2001, ApJ, 546, L123
Cernicharo J., Goicoechea J.R., Benilan Y, 2002, ApJ 580, 157
Cesarsky, C.J. et al. 1996, A&A 315, L32
Cesarsky D., Lequeux J., Ryter C., Gerin, M., 2000a, A&A, 354, L87
Cesarsky D. Jones, A. P., Lequeux J. et al., 2000b, A&A 358,708
Chan K.-W., Roellig T.L., Onada T. et al., 2001, ApJ 546, 273
Cherchneff I., Barker J.R., Tielens A.G.G.M., 1992, ApJ, 401, 269
Chiar, J.E., Tielens A.G.G.M., Whittet D.C.B. et al., 2000, ApJ 537, 749
Chiar, J.E., Tielens A.G.G.M., 2001, ApJ 550, 207
Clegg, P.E. et al. 1996, A&A 315, L38
Cohen M., Tielens A.G.G.M., Allamandola L.J. et al., 1985, ApJ 299, 93
Cohen M., Allamandola L.J., Tielens A.G.G.M. et al., 1986, ApJ 302, 737
Cohen M., Tielens A.G.G.M., Bregman J. et al. 1989, ApJ 341, 246
Cook D.J., Schlemmer S., Balucani N. et al., 1998, J.Phys.Chem. A, 102, 1465
Dartois E., d'Hendecourt L.B., 1997, A&A 323, 534
de Graauw, T. et al. 1996, A&A 315, L49
Désert F.-X., Boulanger F., Puget J.-L., 1990, A&A 237, 215
van Diedenhoven B., Peeters E., van Kerckhoven C. et al., 2004, ApJ 611, 928
van Dishoeck E.F., 2004, submitted to ARAA
Dominik C., Tielens A.G.G.M., 1997, ApJ 480, 647
Draine B.T., Lee H.M., 1984, ApJ 285, 89
Draine B.T., 1989, in *Infrared Spectroscopy in Astronomy*, ed. B.H. Kaldeich, ESA SP-290, 93
Draine B.T., 2003, ARAA 41, 241
Duley W. W., Williams D. A., 1981, MNRAS 196, 269
Dupac X., Bernard J.-P., Boudet N. et al., 2003, A&A 404, L11

Dwek E., Arendt R.G., Fixsen D.J., 1997, ApJ 475, 565
Falgarone E., Panis J.-F., Heithausen A. et al., 1998, A&A 331, 669
Falgarone E., Verstraete L., Pineau des Forts G., Flower D., Puget J.-L., 1999, in *H_2 in Space*, eds. F. Combes & G. Pineau des Forts, Cambridge University Press, 225
Falgarone E., Verstraete L., Pineau des Forts G. et al., 2004, submitted to A&A
Feuchtgruber H., Helmich F.P., van Dishoeck E.F., Wright C. M, 2000, ApJ 535, 111
Förster–Schreiber N.M., Roussel H., Sauvage M., Charmandaris V., 2004, A&A 419, 501
Frenklach M., Feigelson E. D., 1989, ApJ, 341, 372
Gautier T.N. III, Boulanger F., Perault M., Puget J.L., 1992, AJ 103, 1313
Goicoechea J.R., Rodriguez-Fernandez N.J., Cernicharo J, 2004, A&A 600, 214
Gry, C., Swinyard, B., Harwood, A. et al. 2003, 'The ISO Handbook, Volume III: LWS - The Long Wavelength Spectrometer', ESA SP–1262
Gry C., Boulanger F., Nehmé C. et al., 2002, A&A 391, 675
Habart E., Verstraete L., Boulanger F. et al. 2001, A&A 373, 702
Habart E., Boulanger F., Verstraete L., et al. 2003, A&A 397, 623
Habart E., Abergel A., Walmsley M., et al. 2004, submitted to A&A
Harper D.A., Low F.J., Rieke G.H., Thronson H.A. Jr., 1976 ApJ 205, 136
Herbstmeier U., Abraham P., Lemke D. et al., 1998, A&A 332, 739
Herlin N., Bohn I., Reynaud C. et al., 1998, A&A 330, 1127
Hildebrandt R.H., 1983, QJRAS 24, 267
Hollenbach D.J., Tielens A.G.G.M., 1999, Rev. Mod. Phys. 71, 173
Hony S., van Kerckhoven C., Peeters E. et al., 2001, A&A 370, 1030
Hudgins D.M., Allamandola L.J., 1999, ApJ, 516, L41
Hudgins D.M., Bauschlicher C.W., Allamandola L.J., Fetzer J.C., 2000, J. Phys. Chem. A, 104, 3655
Ingalls J.G., Reach W.T., Bania T.M., 2002, ApJ 579, 289
Ingalls J.G., Miville-Deschênes M.A., Reach W.T. et al., ApJ, in press
Joblin C., Abergel A., Bregman J. et al., 2000, in *ISO beyond the peaks: The 2nd ISO workshop on analytical spectroscopy*, Eds. A. Salama, M.F.Kessler, K. Leech & B. Schulz. ESA-SP 456,
Joblin C., Boissel P., & Léger A., 1995, A&A 299, 835
Joblin C., Toublanc D., Boissel P., Tielens A.G.G.M., 2002, Mol. Phys. 100, 3595
Jones A.P., Tielens A.G.G.M., Hollenbach D.J., McKee C.F., 1994, ApJ 433, 797
Jones A.P., Tielens A.G.G.M., Hollenbach D.J., 1996, ApJ 469, 740
Jones A.P., d'Hendecourt L.B., 2000, A&A 355, 1191
Juvela M., Mattila K., Lehtinen K. et al., 2002, A&A, 382, 583
Kahanpää J., Mattila K., Lehtinen K. et al., 2003, A&A 405, 999
Kemper C., Spaans M., Jansen D.J et al. 1999, ApJ 515, 649
Kessler, M.F. et al. 1996, A&A 315, L27
Kessler, M.F., Mller, T.G., Leech, K. et al. 2003, 'The ISO Handbook, Volume I: ISO - Mission & Satellite Overview', ESA SP–1262
Kim H. S., Wagner D. R., Saykally R. J. 2001, Phys. Rev. Lett., 86, 5691
van Kerckhoven C., Hony S., Peeters E. et al. 2000, A&A 357, 1013
Kiss Cs., Abrahm P., Klaas U. et al., 2003, A&A 399, 177
Lagache G., Abergel A., Boulanger F. et al., 1998, A&A 333, 709.
Langhoff S.R., 1996, J. Phys. Chem. 100, 2819
Laureijs R. J., Clark F. O., Prusti T., 1991, ApJ 371, 602
Laureijs R.J., Haikala L., Burgdorf M. et al., 1996, A&A 315, 316

Laureijs, R.J., Klaas, U., Richards, P.J. et al. 2003, 'The ISO Handbook, Volume IV: PHT - The Imaging Photo-Polarimeter', ESA SP–1262
Le Bourlot J., Pineau des Forêts G., Roueff E., Flower D., 1993, A&A 267, 233
Leech, K., Kester, D., Shipman, R. et al. 2003 ESA SP–1262
Léger A., Puget J.L., 1984, A&A 137, L5
Lehtinen K., Lemke D., Mattila K., Haikala L.K., 1998, A&A 333, 702
Lehtinen K., Russeil D., Juvela M. et al., 2004, A&A 423, 975
Lemke, D. et al. 1996, A&A 315, L64
Li A., Draine B.T., 2001, ApJ 554, 778
Li A., Draine B.T., 2002, ApJ 572, 232
Liseau R., White G.J., Larsson B. et al., 1999, A&A 344, 342
Lutz D., Feuchtgruber H., Genzel, R. et al., 1996, A&A 315, 269
Lutz D., Spoon H. W. W., Rigopoulou, D. et al., 1998, ApJ 505, L103
Lutz D., 1999, in *The Universe as Seen by ISO*, Eds. P. Cox & M.F. Kessler, ESA-SP 427 vol.2, 623
Mattila K., Lemke D., Haikala L. K. et al., 1996, A&A, 315, L353
Mathis J.S., Mezger P.G., Panagia N., 1983, A&A 128, 212
Melnick G., Gull G.E., Harwit M., 1979, ApJ 227, 29
Mennella V., Brucato J.R., Colangeli L. et al., 1998, ApJ 496, 1058
Miville-Deschênes M.A., Boulanger F., Joncas G. & Falgarone, E., 2002, A&A 381, 209.
Miville-Deschênes M.A. 2003, in *Chemistry as diagnostic of star formation*, NRC press 363
Miville-Deschênes M.-A., Joncas G., Falgarone E., Boulanger F., 2003, A&A 411, 109
Mizutani M., Onaka T., Shibai H, 2004, A&A 423, 579
Moutou C., Verstraete L., Léger A. et al., 2000, A&A 354, 17
Neufeld D.A., Zmuidzinas J., Schilke P., Phillips T.G., 1997, ApJ 488, 141
Okada Y., Onaka T., Shibai H., Doi Y., 2003, A&A 412, 199
Ossenkopf V., Henning T., 1994, A&A 291, 943.
Pauzat F., Talbi D., Ellinger Y., 1997, A&A 319, 318
Pech C., Joblin C., Boissel P., 2002, A&A 388, 639
Peeters E., Hony S., van Kerckhoven C., Tielens A.G.G.M, 2002, A&A 390, 1089
Peeters E., Allamandola L. J., Bauschlicher C. W. Jr. et al., 2004, ApJ 604, 252
Perault M., Omont A., Simon G. et al., 1996, A&A, 315, 165
Pety J., Teyssier D., Fossé D., 2004, submitted to A&A
Polehampton E.T., Baluteau J.-P., Ceccarelli C., 2002, A&A 388, L44
Preibisch T., Ossenkopf V., Yorke H.W. et al., 1993, A&A 279, 577.
Puget J.-L., Léger A., Boulanger F., 1985, A&A 142, L19
Rachford B.L, Snow T.P., Tumlinson J. et al., 2002, ApJ 577, 221
Rapacioli M., Joblin C., Boissel P., 2004, A&A, in press
Roberts H., Herbst E., 2002, A&A 395, 233
Roche P.F., Aitken D.K., Smith C.H., 1989, MNRAS 236, 485
Roelfsema P., Cox P., Tielens A.G.G.M. et al., 1996, A&A 315, L289
Rosenthal D., Bertoldi F., Drapatz S., 2000, A&A 356, 705
Schutte W.A., Tielens A.G.G.M., Allamandola L.J., 1993, ApJ 415, 397
Schutte W.A., van der Hucht K.A., Whittet D.C.B. et al., 1998, A&A 337, 261
Schneider N., Simon R., Kramer C. et al., 2003, A&A 406, 915
Sellgren K., 1984, ApJ 277, 623
Sellgren K., Allamandola L. J., Bregman J. D. et al., 1985, ApJ 299, 416
Stepnik B., 2001, Thesis, Université of Paris

Stepnik B., Abergel A., Bernard J.-P. et al., 2003, A&A 398, 551
Stepnik B., Abergel A., Jones A.P. et al., 2004, submitted A&A
Szczepanski J., Vala M., 1993, ApJ 414, 646
Teixeira T.C. & Emerson J.P., 1999, A&A 352, 517
Tielens A.G.G.M., Wooden D.H., Allamandola L.J. et al., 1996, ApJ 461, 210
Timmermann R., Köster B., Stutzki J., 1998, A&A 336, L53
Tóth L.V., Hotzel S., Krause O. et al., 2000, A&A, 364, 769
Uchida K.I., Sellgren K., Werner M. W., 1998, ApJ 493, L109
Uchida K.I., Sellgren K., Werner M. W. et al. 2000, ApJ 530, 817
Vastel C., Polehampton E. T., Baluteau J.-P. et al., 2002, ApJ 581, 315
Verstraete L., Puget J.L., Falgarone E. et al., 1996, A&A 315, L337
Verstraete L., Pech C., Moutou C. et al., 2001, A&A 372, 981
Weingartner J.C., Draine B.T., 2001a, ApJS 134, 263
Weingartner J.C., Draine B.T., 2001b, ApJ 548, 296
Weingartner J.C., Draine B.T., 2001c, ApJ 553, 581
Werner et al., submitted to ApJ
Wright C. M., van Dishoeck E.F., Cox P. et al., 1999, ApJ 515, L29